Dyes and Pigments 92 (2012) 1241–1249

Contents lists available at ScienceDirect

Dyes and Pigments

journal homepage: www.elsevier.com/locate/dyepig

Novel 5-benzazolyl-10,15,20-triphenylporphyrins and β,*meso*-benzoxazolyl-bridged porphyrin dyads: Synthesis, characterization and photophysical properties

Satyasheel Sharma, Mahendra Nath*

Department of Chemistry, University of Delhi, Delhi 110 007, India

ARTICLE INFO

Article history:
Received 16 February 2011
Received in revised form
12 July 2011
Accepted 29 July 2011
Available online 5 August 2011

Keywords:
Synthesis
Energy transfer
Fluorescence
meso-Benzazolyl-triphenylporphyrins
β,*meso*-Linked diporphyrins
$La(OTf)_3$

ABSTRACT

Novel 5-benzazolyl-10,15,20-triphenylporphyrins and β,*meso*-benzoxazole-linked diporphyrins were synthesized through $La(OTf)_3$ catalyzed reaction of newly prepared 5-(3,4-diaminophenyl)-10,15,20-triphenylporphyrin or 5-(3-amino-4-hydroxyphenyl)-10,15,20-triphenylporphyrin with aromatic aldehydes in 1,2-dichlorobenzene. On metalation with zinc acetate, freebase β,*meso*-benzoxazole-linked diporphyrin was successfully converted to the Zn–Zn diporphyrin complex in good yield. The synthesized porphyrin analogues were characterized using electronic absorption, IR and ^1H NMR spectroscopy in addition to mass and elemental analyses. The fluorescence studies of 5-benzazolyl-10,15,20-triphenylporphyrins showed efficient intramolecular energy transfer from the pyrene and fluorene subunits to the porphyrin core. In addition, the fluorescence quenching observed in β,*meso*-benzoxazolyl-bridged porphyrin dyads was attributed to the possible nonplanarity of a component of the diporphyrins. The freebase–Ni diporphyrin complex underwent strong emission quenching in comparison to that of freebase diporphyrin and dizinc diporphyrin analogues.

1. Introduction

Porphyrins are a unique class of heteroaromatic macrocyclic ligands that have found wide application in various fields including catalysis [1,2], molecular sensing [3,4], molecular recognition [5,6] and as photosensitizers in photodynamic therapy applications [7–10]. Among various natural pigments, these tetrapyrrole macrocycles have been extensively studied for artificial-light harvesting systems [11–15] and energy or electron-transfer processes [16] due to their high absorption coefficients and rapid excited-state energy transfer characteristics. Thus, these molecules are good candidates for the development of new molecular materials with enhanced photochemical and/or electrochemical properties.

Over the past years, considerable efforts have been made to synthesize porphyrins with extended π-systems [17–23] through peripheral functionalization at the *meso*- and β-positions which can be useful for many applications in a number of areas ranging from photosensitizers to molecular devices for energy and electron-transfer processes. To improve the overall light-harvesting efficiency, various photon harvesting pigments and highly π-conjugated hydrocarbons such as anthraquinone [24], fluorene [25], perylene [26,27], pyrene [28], fluorescein [29] and anthracene [30] have been covalently attached to the easily accessible *meso*-tetraarylporphyrins. Besides these, the porphyrin units have also been linked together in different orientations through *meso-meso*, β-*meso* and β-β positions to modulate the electronic interaction between two porphyrin units within the porphyrin dyads [31–33]. However, a literature survey revealed that the porphyrins with benzazole-ring systems at the *meso*-positions have not been synthesized and evaluated for their optical properties. Therefore, the current work is focused on the synthesis, spectroscopic characterization and photophysical investigation of novel *meso*-substituted benzazolyl-10,15,20-triphenylporphyrins and β,*meso*-benzoxazolyl-bridged diporphyrin systems.

2. Experimental

The reagents and solvents used in this study were purchased from Sigma–Aldrich Chemical Pvt. Ltd., Bangalore, India and Merck Specialities Pvt. Ltd., Mumbai, India. Spectroscopic grade $CHCl_3$ was used to measure UV–Visible absorption and emission spectra of the samples. Thin-layer chromatography (TLC) was conducted on silica gel 60 F_{254} (pre-coated aluminum sheets) from Merck. The products were purified by column chromatography using either activated

* Corresponding author. Tel.: +91 11 27667794x186; fax: +91 11 27666605.
E-mail addresses: mnathchemistry@gmail.com, mnath@chemistry.du.ac.in (M. Nath).

0143-7208/$ – see front matter © 2011 Elsevier Ltd. All rights reserved.
doi:10.1016/j.dyepig.2011.07.022

neutral aluminum oxide (Brokmann grade I–II, Merck) or silica gel (60–120 mesh). ^{1}H NMR spectra were recorded in $CDCl_3$, using a Bruker 300 MHz NMR spectrometer and Jeol ECX 400P (400 MHz) NMR spectrometer. Chemical shifts are expressed in parts per million (ppm) relative to tetramethylsilane as an internal standard. Coupling constants (J) are reported in Hertz (Hz). Elemental analyses for all compounds were performed on Elementar Analysensysteme GmbH VarioEL elemental analyzer. Infrared (IR) spectra of compounds synthesized were recorded on Perkin Elmer IR spectrometer and absorption maxima (υ_{max}) are given in cm^{-1}. Waters LCT Micromass Spectrometer was utilized to obtain the mass spectra of the compounds. UV–Vis absorption and fluorescence spectra were recorded using an Analytik Jena Specord 250 UV–Vis spectrophotometer and a Varian Cary Eclipse fluorescence spectrophotometer, respectively.

2.1. Synthesis of 5-(4-acetamido-3-nitrophenyl)-10,15,20-triphenylporphyrin (**2**)

To a solution of 5-(4-acetamidophenyl)-10,15,20-triphenyl porphyrin **1** (50 mg, 0.074 mmol) in dichloromethane (15 mL), conc. HNO_3 (50 μL) was added. The reaction mixture was stirred at 25 °C for 2 h. After completion of the reaction, the mixture was washed with water and the compound was extracted with chloroform (50 mL). The organic layer was dried over anhydrous sodium sulphate and then evaporated under reduced pressure to obtain the crude product. The title compound was purified on a silica gel column using chloroform/*n*-hexane (80:20) as an eluent. The pure product was obtained as a purple crystalline solid in 75% isolated yield and characterized on the basis of spectral data [34].

2.2. Synthesis of 5-(4-amino-3-nitrophenyl)-10,15,20-triphenylporphyrin (**3**)

A solution of 5-(4-acetamido-3-nitrophenyl)-10,15,20-triphenyl porphyrin **2** (50 mg, 0.069 mmol) in a mixture of TFA (3 mL) and conc. HCl (4 mL) was stirred at 65 °C for 2 h under N_2. After completion of the reaction, the solution was cooled to room temperature and then neutralized with 5% aqueous NaOH solution (50 mL). The desired compound was extracted with chloroform (50 mL). The organic layer was washed thoroughly with water, dried over anhydrous sodium sulphate and the solvent evaporated under reduced pressure. The crude product obtained was purified on a neutral alumina column using chloroform/*n*-hexane (80:20) as eluent. Yield: 95%. ^{1}H NMR (300 MHz, $CDCl_3$) δ = 8.963 (s, 1H, *meso*-ArH), 8.870–8.848 (m, 8H, β-pyrrolic H), 8.222–8.205 (m, 7H, *meso*-ArH), 7.767–7.469 (m, 9H, *meso*-ArH), 7.115 (d, J = 8.4 Hz, 1H, *meso*-ArH), 6.378 (s, 2H, NH_2), −2.781 (s, 2H, internal NH) ppm. IR (Film) ν/cm^{-1}: 3492, 3381, 3320, 1630, 1595, 1559, 1517, 1473, 1345, 1252, 1170, 1074, 968, 800, 749, 701. ESI-MS: m/z = 674 $(M)^+$. Anal. Calcd. for $C_{44}H_{30}N_6O_2.2H_2O$: C, 74.35; H, 4.82; N, 11.82. Found: C, 74.06; H, 5.40; N, 11.95.

2.3. Synthesis of 5-(3,4-diaminophenyl)-10,15,20-triphenylporphyrin (**4**)

To a solution of 5-(4-amino-3-nitrophenyl)-10,15,20-triphenyl porphyrin **3** (50 mg, 0.074 mmol) in conc. HCl (10 mL), $SnCl_2 \cdot 2H_2O$ (100 mg, 0.44 mmol) was added. The reaction mixture was stirred at 65 °C for 2 h under an inert atmosphere. After completion of the reaction, the mixture was allowed to cool at room temperature, neutralized with 10% aqueous NaOH solution and extracted with chloroform (50 mL). The organic layer was washed thoroughly with water, dried over anhydrous sodium sulphate and evaporated to dryness under reduced pressure. The crude product was purified by column chromatography on activated neutral alumina using chloroform as eluent. Yield: 75% (purple crystalline solid). ^{1}H NMR (300 MHz, $CDCl_3$) δ = 8.974 (d, J = 4.8 Hz, 2H, β-pyrrolic H), 8.817 (d, J = 4.8 Hz, 6H, β-pyrrolic H), 8.221–8.196 (m, 6H, *meso*-ArH), 7.773–7.756 (m, 9H, *meso*-ArH), 7.581–7.550 (m, 2H, *meso*-ArH), 7.055 (d, J = 7.8 Hz, 1H, *meso*-ArH), 3.683 (brs, 4H, $2NH_2$), −2.762 (s, 2H, internal NH) ppm. IR (Film) ν/cm^{-1}: 3421, 3321, 1620, 1595, 1472, 1440, 1350, 1219, 1155, 1070, 969, 800, 751, 701. ESI-MS: m/z = 645 $(M + H)^+$. Anal. Calcd. for $C_{44}H_{32}N_6$: C, 81.96; H, 5.00; N, 13.03. Found: C, 82.08; H, 4.84; N, 12.96.

2.4. General procedure for the synthesis of meso-substituted benzimidazolyl-triphenylporphyrins (**8a–e**)

To a solution of 5-(3,4-diaminophenyl)-10,15,20-triphenyl porphyrin **4** (30 mg, 0.046 mmol) in 1,2-dichlorobenzene (10 mL), the aryl aldehyde (0.069 mmol) was added followed by the addition of $La(OTf)_3$ (5 mg, 0.009 mmol). The reaction mixture was stirred at 100 °C for 8 h. The progress of the reaction was monitored by TLC. After completion of the reaction, the mixture was cooled to room temperature and loaded onto a silica gel column. The column was firstly eluted with *n*-hexane to remove 1,2-dichlorobenzene and then with chloroform to afford the desired product as a purple crystalline solid in 78–85% isolated yields.

2.4.1. 5-[2-(4-Chlorophenyl)-1H-benzimidazol-5-yl]-10,15,20-triphenylporphyrin (**8a**)

The compound **8a** was prepared from compound **4** (30 mg, 0.046 mmol) and 4-chlorobenzaldehyde (9.8 mg, 0.069 mmol) according to the general procedure given earlier. Yield: 80%. ^{1}H NMR (300 MHz, $CDCl_3$) δ = 8.840–8.805 (m, 9H, β-pyrrolic H & *meso*-ArH), 8.225–8.173 (m, 7H, *meso*-ArH), 8.087 (s, 1H, NH), 7.915 (d, J = 7.8 Hz, 2H, ArH), 7.758–7.719 (m, 10H, *meso*-ArH), 7.406 (d, J = 6.9 Hz, 2H, ArH), −2.738 (s, 2H, internal NH) ppm. IR (Film) ν/cm^{-1}: 3317, 1597, 1473, 1441, 1350, 1219, 1095, 968, 835, 800, 729, 701. ESI-MS: m/z = 764 $(M)^+$. Anal. Calcd. for $C_{51}H_{33}ClN_6.3H_2O$: C, 74.76; H, 4.80; N, 10.26. Found: C, 75.15; H, 4.57; N, 9.85.

2.4.2. 5-[2-(Naphthalen-1-yl)-1H-benzimidazol-5-yl]-10,15,20-triphenylporphyrin (**8b**)

The compound **8b** was prepared from compound **4** (30 mg, 0.046 mmol) and 2-naphthaldehyde (10.8 mg, 0.069 mmol) according to the general procedure given earlier. Yield: 82%. ^{1}H NMR (400 MHz, $CDCl_3$) δ = 8.849–8.826 (m, 6H, β-pyrrolic H), 8.796 (d, J = 4.7 Hz, 2H, β-pyrrolic H), 8.609 (s, 1H, *meso*-ArH), 8.224–8.137 (m, 9H, *meso*-ArH & NH), 7.946–7.831 (m, 3H, ArH), 7.757–7.724 (m, 11H, *meso*-ArH & ArH), 7.507 (t, J = 7.3 Hz, 2H, ArH), −2.734 (s, 2H, internal NH) ppm. IR (Film) ν/cm^{-1}: 3312, 1595, 1440, 1350, 1261, 1072, 969, 800, 751, 700. ESI-MS: m/z = 780 $(M)^+$. Anal. Calcd. for $C_{55}H_{36}N_6$: C, 84.59; H, 4.65; N, 10.76. Found: C, 84.29; H, 4.98; N; 10.56.

2.4.3. 5-[2-(Pyren-1-yl)-1H-benzimidazol-5-yl]-10,15,20-triphenylporphyrin (**8c**)

The compound **8c** was prepared from compound **4** (30 mg, 0.046 mmol) and 1-pyrenecarboxaldehyde (15.9 mg, 0.069 mmol) according to the general procedure given earlier. Yield: 85%. ^{1}H NMR (400 MHz, $CDCl_3$) δ = 8.927 (d, J = 9.1 Hz, 1H, ArH), 8.879–8.848 (m, 4H, β-pyrrolic H), 8.714 (d, J = 4.5 Hz, 2H, β-pyrrolic H), 8.635 (d, J = 4.5 Hz, 2H, β-pyrrolic H), 8.320–8.169 (m, 8H, *meso*-ArH & NH), 7.960 (d, J = 7.7 Hz, 1H, *meso*-ArH), 7.902 (d, J = 9.4 Hz, 1H, ArH), 7.817–7.687 (m, 13H, *meso*-ArH & ArH), 7.460 (t, J = 7.7 Hz, 1H, ArH), 7.321 (d, J = 7.0 Hz, 1H, ArH), 7.056–6.984 (m, 2H, ArH), −2.846 (s, 2H, internal NH) ppm. IR (Film) ν/cm^{-1}: 3318, 1597, 1350, 1218, 969, 846, 801, 753. ESI-MS:

$m/z = 854$ $(M)^+$. Anal. Calcd. for $C_{61}H_{38}N_6$: C, 85.69; H, 4.48; N, 9.83. Found: C, 85.46; H, 4.76; N; 10.17.

2.4.4. 5-[2-(9H-fluoren-2-yl)-1H-benzimidazol-5-yl]-10,15,20-triphenylporphyrin (**8d**)

The compound **8d** was prepared from compound **4** (30 mg, 0.046 mmol) and fluorene-2-carboxaldehyde (13.4 mg, 0.069 mmol) according to the general procedure given earlier. Yield: 78%. ^{1}H NMR (300 MHz, $CDCl_3$) $\delta = 8.832–8.765$ (m, 8H, β-pyrrolic H), 8.375 (s, 1H, NH), 8.300 (s, 1H, *meso*-ArH), 8.180 (d, $J = 6.6$ Hz, 6H, *meso*-ArH), 8.069 (d, $J = 7.2$ Hz, 1H, *meso*-ArH), 7.946 (d, $J = 7.2$ Hz, 1H, *meso*-ArH), 7.750–7.706 (m, 12H, *meso*-ArH & ArH), 7.420 (d, $J = 6.9$ Hz, 1H, ArH), 7.291–7.245 (m, 3H, ArH), 3.809 (s, 2H, CH_2), −2.751 (s, 2H, internal NH) ppm. IR (Film) ν/cm^{-1}: 3317, 1594, 1441, 1350, 1219, 1072, 969, 939, 801, 734, 701. ESI-MS: $m/z = 819$ $(M + H)^+$. Anal. Calcd. for $C_{58}H_{38}F_3N_6.0.5H_2O$: C, 77.31; H, 4.24; N, 10.40. Found: C, 77.22; H, 4.60; N; 10.08.

2.4.5. 5-[2-(4-Trifluoromethylphenyl)-1H-benzimidazol-5-yl]-10,15,20-triphenylporphyrin (**8e**)

The compound **8e** was prepared from compound **4** (30 mg, 0.046 mmol) and 4-trifluoromethylbenzaldehyde (12 mg, 0.069 mmol) according to the general procedure given earlier. Yield: 85%. ^{1}H NMR (400 MHz, $CDCl_3$) $\delta = 8.844–8.807$ (m, 9H, β-pyrrolic H & ArH), 8.226–8.181 (m, 7H, *meso*-ArH), 8.127–8.109 (m, 3H, ArH & NH), 7.783–7.725 (m, 12H, *meso*-ArH & ArH), −2.7534 (s, 2H, internal NH) ppm. IR (Film) ν/cm^{-1}: 3317, 1596, 1474, 1441, 1351, 1219, 1092, 963, 835, 800, 729, 700. ESI-MS: $m/z = 798$ $(M)^+$. Anal. Calcd. for $C_{52}H_{33}F_3N_6.1.5H_2O$: C, 75.62; H, 4.39; N, 10.18. Found: C, 75.08; H, 4.53; N, 10.03.

2.5. Synthesis of 5-(4-hydroxy-3-nitrophenyl)-10,15,20-triphenylporphyrin (**6**)

To a solution of 5-(4-hydroxyphenyl)-10,15,20-triphenylporphyrin **5** (50 mg, 0.079 mmol) in dichloromethane (10 mL), conc. HNO_3 (60 μL) was added slowly and the mixture was stirred at 25 °C for 15 min. Then the reaction was quenched with water (20 mL) and compound was extracted with chloroform (2 × 20 mL). The organic layers were combined, washed thoroughly with water and dried over anhydrous sodium sulphate. On evaporation of the solvent under reduced pressure, the crude product obtained was purified by column chromatography on silica gel using chloroform/*n*-hexane (80:20) as solvent. The purple crystalline product was obtained in 90% isolated yield and characterized on the basis of spectral data as reported in the literature [34].

2.6. Synthesis of 5-(3-amino-4-hydroxyphenyl)-10,15,20-triphenylporphyrin (7)

To a solution of 5-(4-hydroxy-3-nitrophenyl)-10,15,20-triphenyl porphyrin **6** (50 mg, 0.074 mmol) in conc. HCl (10 mL), $SnCl_2 \cdot 2H_2O$ (100 mg, 0.44 mmol) was added. The reaction mixture was stirred at 65 °C for 2 h under an inert atmosphere. On completion of the reaction, the mixture was allowed to cool at 25 °C and then neutralized with 5% aqueous sodium hydroxide solution. The title compound was extracted with chloroform (3 × 30 mL). The organic layers were combined, washed thoroughly with water, dried over sodium sulphate and evaporated to dryness under reduced pressure. The crude product obtained was purified by column chromatography on silica gel using 5% methanol in chloroform as eluent. Yield: 85%. ^{1}H NMR (300 MHz, $CDCl_3$) $\delta = 8.936$ (s, 1H, *meso*-ArH), 8.828 (s, 8H, β-pyrrolic H), 8.203 (s, 7H, *meso*-ArH), 7.749 (s, 10H, *meso*-ArH), 5.104 (brs, 1H, OH), 4.069 (brs, 2H, NH_2), −2.769 (s, 2H, internal NH) ppm. IR (Film) ν/cm^{-1}: 3374, 3312, 1597, 1472, 1439, 1350, 1276, 1217, 1139, 1070, 969, 871, 799, 727, 700. ESI-MS: $m/z = 646$ $(M + H)^+$. Anal. Calcd. for $C_{44}H_{31}N_5O.H_2O$: C,79.62; H, 5.01; N, 10.55. Found: C, 79.54; H, 5.34; N; 10.36.

2.7. General procedure for the synthesis of meso-substituted benzoxazolyl-triphenylporphyrins (**9a**–**d**)

To a solution of 5-(3-amino-4-hydroxyphenyl)-10,15,20-triphenylporphyrin **7** (30 mg, 0.046 mmol) in 1,2-dichlorobenzene (10 mL), the aryl aldehyde (0.069 mmol) was added followed by the addition of $La(OTf)_3$ (5 mg, 0.009 mmol). The reaction mixture was heated at 160 °C under stirring for 16 h. After completion of the reaction, the mixture was allowed to cool at room temperature and then directly loaded onto a silica gel column. 1,2-Dichlorobenzene was removed on elution with *n*-hexane and the desired product was eluted from the column using chloroform.

2.7.1. 5-[2-(4-Chlorophenyl)benzoxazol-5-yl]-10,15,20-triphenylporphyrin (**9a**)

The compound **9a** was prepared from compound **7** (30 mg, 0.046 mmol) and 4-chlorobenzaldehyde (9.8 mg, 0.069 mmol) according to the general procedure given earlier. Yield: 68%. ^{1}H NMR (300 MHz, $CDCl_3$) $\delta = 8.849$ (s, 8H, β-pyrrolic H), 8.618 (s, 1H, *meso*-ArH), 8.338 (d, $J = 7.2$ Hz, 2H, ArH), 8.226–8.213 (m, 7H, *meso*-ArH), 7.904 (d, $J = 8.4$ Hz, 1H, *meso*-ArH), 7.763 (s, 9H, *meso*-ArH), 7.576 (d, $J = 7.2$ Hz, 2H, ArH), −2.746 (s, 2H, internal NH) ppm. IR (Film) ν/cm^{-1}: 3317, 1595, 1560, 1465, 1440, 1352, 1260, 1188, 969, 864, 800, 752, 700. ESI-MS: $m/z = 765$ $(M)^+$. Anal. Calcd. for $C_{51}H_{32}ClN_5O.1.5H_2O$: C, 77.21; H, 4.45; N, 8.83. Found: C, 76.87; H, 4.57; N, 8.22.

2.7.2. 5-[2-(Naphthalen-1-yl)benzoxazol-5-yl]-10,15,20-triphenylporphyrin (**9b**)

The compound **9b** was prepared from compound **7** (30 mg, 0.046 mmol) and 2-naphthaldehyde (10.8 mg, 0.069 mmol) according to the general procedure given earlier. Yield: 70%. ^{1}H NMR (400 MHz, $CDCl_3$) $\delta = 8.939$ (s, 1H, *meso*-ArH), 8.869–8.863 (d, $J = 2.2$ Hz, 8H, β-pyrrolic H), 8.679 (d, $J = 1.2$ Hz, 1H, ArH), 8.459 (dd, $J_1 = 8.8$ Hz, $J_2 = 1.6$ Hz, 1H, *meso*-ArH), 8.244–8.224 (m, 7H, *meso*-ArH), 8.036 (d, $J = 8.0$ Hz, 2H, ArH), 7.956 (d, $J = 8.0$ Hz, 2H, ArH), 7.769–7.754 (d, 9H, *meso*-ArH), 7.613 (t, $J = 4.0$ Hz, 2H, ArH), −2.734 (s, 2H, internal NH) ppm. IR (Film) ν/cm^{-1}: 3318, 1597, 1560, 1468, 1441, 1350, 1260, 1184, 967, 860, 801, 752, 701. ESI-MS: $m/z = 781$ $(M)^+$. Anal. Calcd. for $C_{55}H_{35}N_5O$: C, 85.59; H, 4.36; N, 8.18. Found: C, 85.46; H, 4.71; N, 8.33.

2.7.3. 5-[2-(Pyren-1-yl)benzoxazol-5-yl]-10,15,20-triphenylporphyrin (**9c**)

The compound **9c** was prepared from compound **7** (30 mg, 0.046 mmol) and 1-pyrenecarboxaldehyde (15.9 mg, 0.069 mmol) according to the general procedure given earlier. Yield: 75%. ^{1}H NMR (400 MHz, $CDCl_3$) $\delta = 9.963$ (d, $J = 9.4$ Hz, 1H, ArH), 9.071 (d, $J = 8.0$ Hz, 1H, ArH), 8.922–8.861 (m, 8H, β-pyrrolic H), 8.802 (d, $J = 1.2$ Hz, 1H, *meso*-ArH), 8.361–8.314 (m, 13H, *meso*-ArH & ArH), 8.083 (t, $J = 7.7$ Hz, 1H, ArH), 8.035 (d, $J = 8.0$ Hz, 1H, ArH), 7.776–7.764 (m, 9H, *meso*-ArH), −2.739 (s, 2H, internal NH) ppm. IR (Film) ν/cm^{-1}: 3317, 1594, 1558, 1473, 1439, 1349, 1256, 1188, 1073, 967, 842, 797, 699. ESI-MS: $m/z = 855$ $(M)^+$. Anal. Calcd. for $C_{61}H_{37}N_5O.H_2O$: C, 83.83; H, 4.50; N, 8.01. Found: C, 84.09; H, 5.05; N, 7.53.

2.7.4. 5-[2-(9H-fluoren-2-yl)benzoxazol-5-yl]-10,15,20-triphenylporphyrin (**9d**)

The compound **9d** was prepared from compound **7** (30 mg, 0.046 mmol) and fluorene-2-carboxaldehyde (13.4 mg, 0.069 mmol)

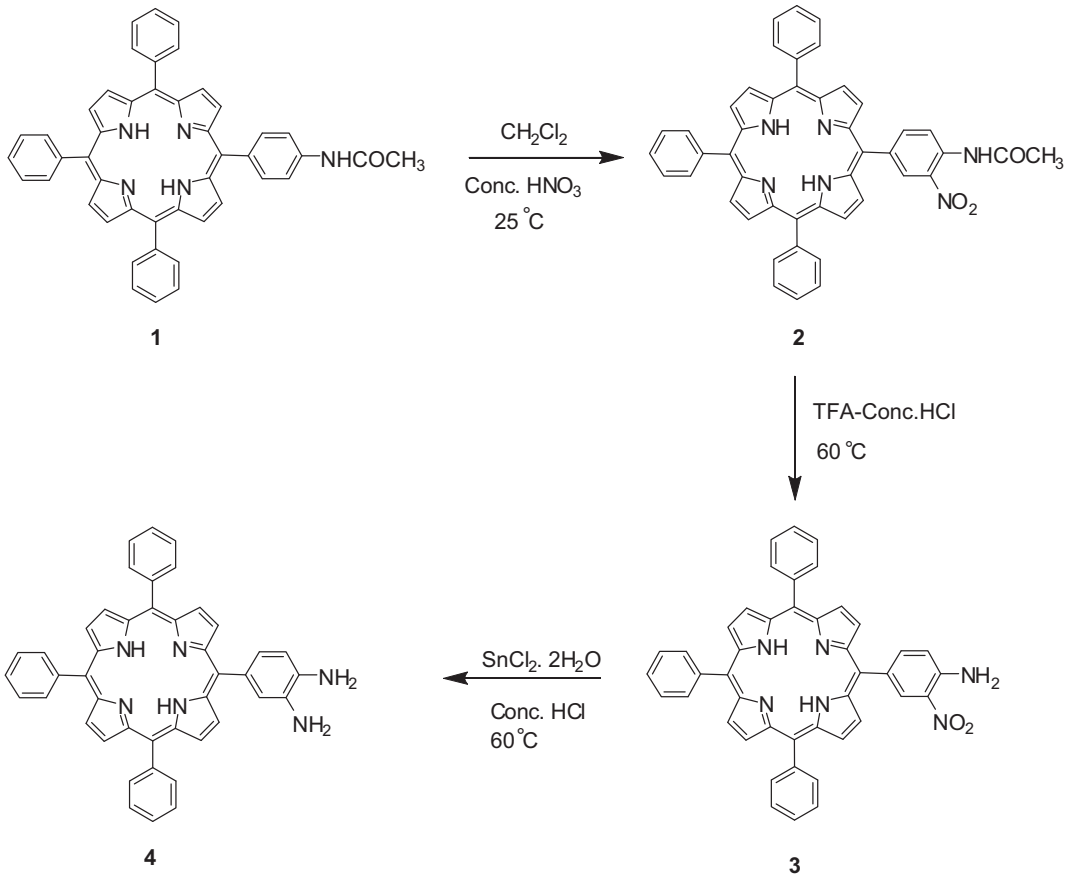

Scheme 1. Synthesis of 5-(3,4-diaminophenyl)-10,15,20-triphenylporphyrin.

according to the general procedure given earlier. Yield: 72%. ^{1}H NMR (400 MHz, $CDCl_3$) $\delta = 8.856$ (s, 8H, β-pyrrolic H), 8.631 (s, 1H, *meso*-ArH), 8.601 (s, 1H, ArH), 8.460 (d, $J = 8.0$ Hz, 1H, ArH), 8.235–8.187 (m, 7H, *meso*-ArH), 7.999 (d, $J = 8.0$ Hz, 1H, ArH), 7.914 (t, $J = 8.0$ Hz, 2H, ArH), 7.766–7.751 (m, 9H, *meso*-ArH), 7.631 (d, $J = 6.8$ Hz, 1H, *meso*-ArH), 7.460–7.403 (m, 2H, ArH), 4.078 (s, 2H, CH_2), −2.739 (s, 2H, internal NH) ppm. IR (Film) ν/cm^{-1}: 3317, 1595, 1441, 1350, 1217, 1072, 968, 939, 801, 730, 701. ESI-MS: $m/z = 819$ $(M)^+$. Anal. calcd. for $C_{58}H_{37}N_5O.H_2O$: C, 83.13; H, 4.69; N, 8.36. Found: C, 83.09; H, 4.81; N, 8.01.

2.8. Synthesis of β,meso-benzoxazolyl-bridged porphyrin dyads (*11a and 11b*)

To a solution of 5-(3-amino-4-hydroxyphenyl)-10,15,20-triphenylporphyrin **7** (50 mg, 0.077 mmol) in 1,2-dichlorobenzene (10 mL), β-formyl-5,10,15,20-tetraphenylporphyrin **10a** or nickel(II) β-formyl-5,10,15,20-tetraphenylporphyrin **10b** (0.077 mmol) was added followed by the addition of $La(OTf)_3$ (9 mg, 0.015 mmol). The reaction mixture was stirred at 160 °C for 16 h and then allowed to cool at 25 °C. The reaction mixture was directly loaded onto a silica-gel column. The column was firstly eluted with hexane to remove 1,2-dichlorobenzene and then after with chloroform to afford compound **11a** or **11b**.

2.8.1. 2-[5-(10,15,20-triphenylporphyrin-5-yl)-benzoxazol-2-yl]-5,10,15,20-tetraphenylporphyrin (*11a*)

Yield: 55%. ^{1}H NMR (400 MHz, $CDCl_3$) $\delta = 9.439$ (s, 1H, β-pyrrolic H), 8.967–8.882 (m, 12H, β-pyrrolic H), 8.798 (s, 2H, β-pyrrolic H), 8.563 (s, 1H, *meso*-ArH), 8.350 (d, $J = 7.38$ Hz, 2H, *meso*-ArH), 8.316–8.234 (m, 12H, *meso*-ArH), 8.136 (dd, $J_1 = 8.0$ Hz, $J_2 = 1.7$ Hz, 1H, *meso*-ArH), 7.932–7.766 (m, 18H, *meso*-ArH), 7.611–7.555 (m, 3H, *meso*-ArH), 7.496 (d, $J = 7.7$ Hz, 1H, *meso*-ArH), −2.519 (s, 2H, internal NH), −2.694 (s, 2H, internal NH) ppm. IR (Film) ν/cm^{-1}: 3320, 1597, 1469, 1441, 1350, 1260, 1219, 1178, 1072, 1002, 966, 800, 753, 700. ESI-MS: $m/z = 1267$ $(M)^+$. Anal. Calcd. for $C_{89}H_{57}N_9O.H_2O$: C, 83.09; H, 4.62; N, 9.80. Found: C, 82.95; H, 4.97; N, 9.53.

2.8.2. Nickel(II) 2-[5-(10,15,20-triphenylporphyrin-5-yl)-benzoxazol-2-yl]-5,10,15,20-tetraphenylporphyrin (*11b*)

Yield: 45%. ^{1}H NMR (400 MHz, $CDCl_3$) $\delta = 9.357$ (s, 1H, β-pyrrolic H), 8.933 (d, $J = 4.0$ Hz, 2H, β-pyrrolic H), 8.864 (s, 6H, β-pyrrolic H), 8.799 (d, $J = 5.0$ Hz, 1H, β-pyrrolic H), 8.761 (d, $J = 4.7$ Hz, 1H, β-pyrrolic H), 8.724–8.695 (m, 3H, β-pyrrolic H), 8.600 (d, $J = 4.6$ Hz, 1H, β-pyrrolic H), 8.537 (s, 1H, *meso*-ArH), 8.261–8.210 (m, 6H, *meso*-ArH), 8.100–8.021 (m, 8H, *meso*-ArH), 7.786–7.677 (m, 19H, *meso*-ArH), 7.506–7.411 (m, 4H, *meso*-ArH), −2.714 (s, 2H, internal NH) ppm. IR (Film) ν/cm^{-1}: 3317, 1597, 1464, 1441, 1350, 1259, 1219, 1178, 1072, 1002, 966, 800, 754, 700. ESI-MS: $m/z = 1324$ $(M + H)^+$.

2.9. Synthesis of di-zinc(II) 2-[5-(10,15,20-triphenylporphyrin-5-yl)-benzoxazol-2-yl]-5,10,15,20-tetraphenylporphyrin (*11c*)

To the solution of freebase–freebase diporphyrin **11a** (10 mg, 0.008 mmol) in dichloromethane (5 mL), a solution of $Zn(OAc)_2 \cdot 2H_2O$ (6 mg, 0.027 mmol) in methanol (0.5 mL) was added and the reaction mixture was stirred at room temperature for 30 min. After completion of the reaction, the mixture was diluted with dichloromethane (20 mL) and washed with water (3 × 25 mL).

The organic layer was dried over sodium sulphate and evaporated to dryness under vacuum. The residue obtained was subjected to column chromatography on silica gel using $CHCl_3$ as eluent. The pure product was obtained after eluting the column with 5% MeOH in chloroform in 80% yield. ^{1}H NMR (400 MHz, $CDCl_3$ + DMSO-d_6) $\delta = 9.195$ (s, 1H, β-pyrrolic H), 9.069 (d, $J = 4.7$ Hz, 2H, β-pyrrolic H), 8.980–8.685 (m, 12H, β-pyrrolic H), 8.317–8.218 (m, 10H, *meso*-ArH), 8.035 (s, 4H, *meso*-ArH), 7.825–7.752 (m, 18H, *meso*-ArH), 7.568–7.416 (m, 4H. *meso*-ArH), 7.272–7.251 (m, 2H, *meso*-ArH) ppm. IR (Film) ν/cm^{-1}: 1597, 1462, 1265, 1070, 994, 795, 754, 699. ESI-MS: $m/z = 1392$ $(M + H)^+$. Anal. Calcd. for $C_{89}H_{53}N_9Zn_2O.2H_2O$: C, 74.69; H, 4.01; N, 8.81. Found: C, 74.50; H, 4.39; N, 8.64.

3. Results and discussion

3.1. Synthesis and structure characterization

The novel 5-benzazolyl-10,15,20-triphenylporphyrins (**8a**–**e** and **9a**–**d**) and β,*meso*-benzoxazolyl-bridged diporphyrins (**11a**–**c**) were synthesized as outlined in schemes 3 and 4. For the synthesis of these porphyrin derivatives, two new precursors, 5-(3,4-diaminophenyl)-10,15,20-triphenylporphyrin (**4**) and 5-(3-amino-4-hydroxyphenyl)-10,15,20-triphenylporphyrin (**7**) were prepared through regioselective functionalization of 5-(4-acetamidophenyl)-10,15,20-triphenyl porphyrin (**1**) and 5-(4-hydroxyphenyl)-10,15,20-triphenylporphyrin (**5**), respectively as shown in schemes 1 and 2. First, 5-(4-acetamido phenyl)-10,15,20-triphenylporphyrin was synthesized from easily accessible *meso*-tetraphenylporphyrins by following the literature procedure [34]. The regiospecific phenyl nitration of this porphyrin (**1**) by using conc. HNO_3 in CH_2Cl_2 under modified reaction conditions at 25 °C afforded 5-(4-acetamido-3-nitrophenyl)-10,15,20-triphenyl porphyrin (**2**) in 70% isolated yield. On deprotection of the acetamido group using TFA-conc. HCl mixture at 65 °C, porphyrin (**2**) was converted to the corresponding 5-(4-amino-3-nitrophenyl)-10,15,20-triphenylporphyrin (**3**) which on treatment with $SnCl_2 \cdot 2H_2O$ in conc. HCl at 65 °C for 2 h under nitrogen atmosphere afforded 5-(3,4-diaminophenyl)-10,15,20-triphenylporphyrin (**4**). After purification of the crude product by column chromatography on neutral alumina, porphyrin (**4**) was obtained in 75% isolated yield. Similarly, another novel starting material, 5-(3-amino-4-hydroxyphenyl)-10,15,20-triphenylporphyrin (**7**) was synthesized from 5-(4-hydroxyphenyl)-10,15,20-triphenylporphyrin (**5**) [35] via nitration by conc. HNO_3 followed by reduction of the nitro substituent under standard $SnCl_2$/HCl conditions as shown in Scheme 2. After purification on silica gel, porphyrin **7** was obtained in 85% isolated yield. These porphyrins **4** and **7** were characterized spectroscopically and used as precursors for the preparation of novel *meso*-substituted benzazolyl-triphenyl porphyrins (**8a**–**e** and **9a**–**d**) and β,*meso*-benzoxazolyl-bridged porphyrin dyads (**11a,b**), respectively.

The *meso*-substituted benzimidazolyl-triphenylporphyrins (**8a**–**e**) were synthesized in 75–85% isolated yields by condensation

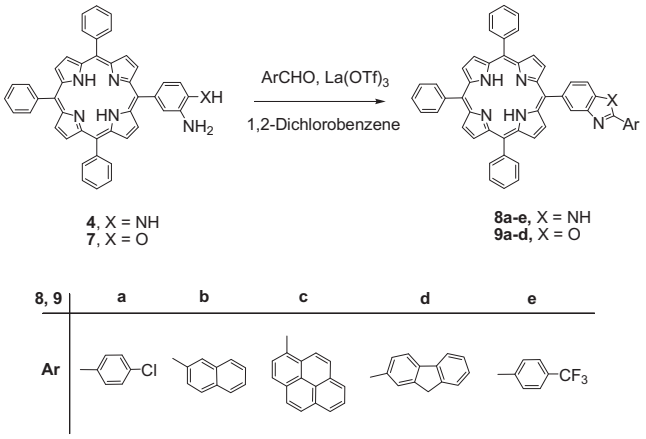

Scheme 3. Synthesis of *meso*-substituted benzazolyl-triphenylporphyrins.

cyclization of 5-(3,4-diaminophenyl)-10,15,20-triphenylporphyrin (**4**) with 1.5 equivalents of aryl aldehydes in 1,2-dichlorobenzene using $La(OTf)_3$ as a Lewis acid catalyst at 100 °C temperature for 8 h. In contrast, *meso*-substituted benzoxazolyl-triphenylporphyrins (**9a**–**d**) were synthesized similarly from 5-(3-amino-4-hydroxy phenyl)-10,15,20-triphenylporphyrin (**7**) at 160 °C temperature in 68–75% isolated yields (Scheme 3). In absence of $La(OTf)_3$, the reaction only proceeded at high temperature (>180 °C) and produced desired products in low yields due to the formation of side products. The reaction seems to proceed through initial formation of an iminoporphyrin intermediate, which was possibly activated in the presence of $La(OTf)_3$, and thus facilitates the intramolecular oxidative cyclization to afford desired products in good yields.

Furthermore, this synthetic protocol was extended to obtain novel β,*meso*-linked diporphyrin systems (**11a**–**c**) with a benzoxazole spacer as shown in Scheme 4. The freebase–freebase diporphyrin (**11a**) and freebase–nickel(II) diporphyrin (**11b**) were synthesized in moderate yields at 160 °C by the reaction of porphyrin **7** with 2-formyl-5,10,15,20-tetraphenyl-porphyrin (**10a**) and nickel(II) 2-formyl-5,10,15,20-tetraphenylporphyrin (**10b**), respectively in the presence of a catalytic amount of $La(OTf)_3$ in 1,2-dichlorobenzene. The zinc–zinc diporphyrin analogue (**11c**) was prepared from freebase–freebase diporphyrin (**11a**) via zinc insertion reaction using $Zn(OAc)_2 \cdot 2H_2O$ in dichloromethane–MeOH mixture at 25 °C (Scheme 4).

All the newly synthesized compounds **3**, **4**, **7**, **8a**–**e**, **9a**–**d** and **11a**–**c** were purified by column chromatography and characterized on the basis of ^{1}H NMR, IR, UV–Vis and mass spectral data. The ^{1}H NMR of porphyrins **3**, **4**, **7**, **8a**–**e** and **9a**–**d** showed a characteristic singlet at about $\delta = -2.7$ ppm for the NH protons of the porphyrin core. The characteristic β-pyrrolic protons appeared in the downfield region between $\delta = 8.6$–8.9 ppm. In the case of *meso*-substituted benzimidazolyl porphyrins (**8a**–**e**), the NH proton of

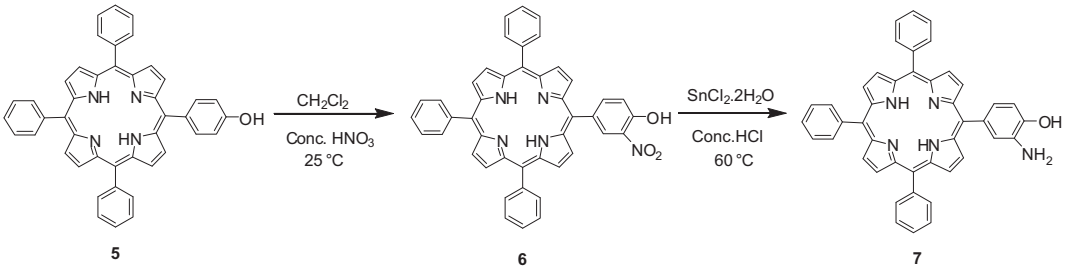

Scheme 2. Synthesis of 5-(3-amino-4-hydroxyphenyl)-10,15,20-triphenylporphyrin.

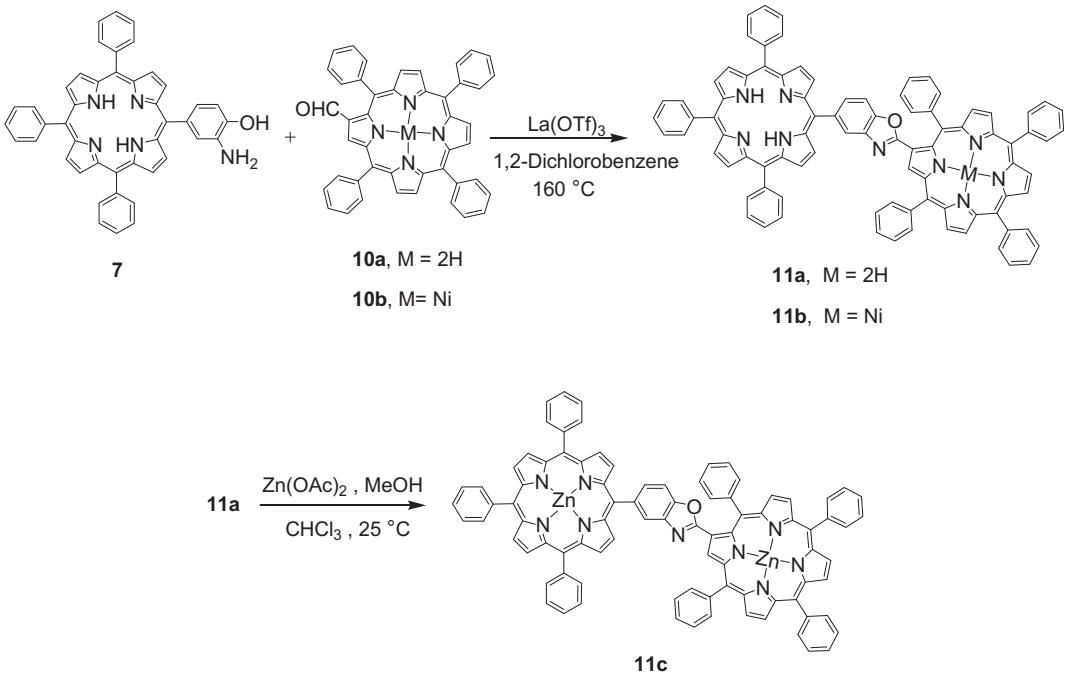

Scheme 4. Synthesis of *β*,*meso*-benzoxazolyl-bridged porphyrin dyads.

the benzimidazole ring was present as a singlet between $\delta = 8.0–8.3$ ppm. In addition, porphyrins **8d** and **9d** showed a characteristic singlet for the CH_2 protons of the fluorenyl moiety at $\delta = 3.8$ and 4.0 ppm, respectively. In contrast, the proton NMR of freebase–freebase diporphyrin (**11a)** showed a characteristic peak for the *β*-proton adjacent to the benzoxazole moiety as a singlet at $\delta = 9.43$ ppm. The remaining 14 *β*-pyrrolic protons appeared as a multiplet at $\delta = 8.82–8.96$ ppm for 12 protons and a singlet at $\delta = 8.79$ ppm for 2 protons, respectively. A singlet at $\delta = 8.56$ ppm for one proton was assigned to the *ortho*-position of the *meso*-phenyl ring. The remaining 37 *meso*-phenyl protons appeared either as doublets or multiplets between $\delta = 7.49–8.35$ ppm. The two singlets at $\delta = -2.51$ and -2.69 ppm for two protons each were assigned to the internal NH for the two porphyrin rings. The IR spectrum of diporphyrin (**11a**) showed a peak at 3320 cm^{-1} due to the NH bond stretching. The structure of dyad (**11a**) was further supported by the mass, which showed molecular ion peak $(M)^+$ at *m*/*z* 1267. Similarly, porphyrin dyads **11b**–**c** were characterized and their spectral data are presented in the experimental section.

3.2. Photophysical properties

The electronic absorption and emission data of the newly synthesized compounds are presented in Table 1. The *meso*-benzazolyl-triphenylporphyrins (**8a**–**e** and **9a**–**d)** exhibited typical intense Soret- or B-bands at ~421 nm and four weaker Q bands at ~517, 552, 592 and 647 nm. The UV–Vis spectra of porphyrins **4**, **7**, **8c**, **8d**, **9c** and **9d** are shown in Fig. 1a. Besides the Soret and Q bands in porphyrins (**8c**–**d** and **9c**–**d**), an additional absorption peak originates from the presence of pyrenyl and fluorenyl units at 280 nm and 320 nm, respectively. Thus, the absorption spectra of these compounds showed the features of both porphyrin and pyrene or fluorene subunits and suggest that there is no substantial interaction between the attached moiety and the porphyrin ring in the ground state. This observation is in agreement with a nearly perpendicular orientation of the aryl group relative to the porphyrin plane in the freebase *meso*-tetraarylporphyrins [36].

The electronic absorption spectra of *β*,*meso*-benzoxazolyl-bridged porphyrin dyads (**11a**–**c)** are shown in Fig. 1b. The visible absorption spectra of porphyrin dyads displayed an intense Soret-band with slight splitting at 421, 428 nm for freebase–freebase

Table 1
Electronic absorption and emission data for porphyrins **3, 4, 7, 8a**–**e, 9a**–**d** and **11a**–**c**.

Compd no.	Absorption[a] λ_{max}, nm ($\varepsilon \times 10^{-4}$, M^{-1} cm^{-1})	Fluorescence[a,b] (λ_{em}/nm)
3	422(47.33), 518(2.01), 551(1.04), 592(0.58), 648(0.26)	652, 717
4	422(48.90), 518(2.57), 555(1.26), 594(0.68), 650(0.59)	655, 719
7	421(46.33), 518(2.35), 552(1.02), 591(0.70), 648(0.51)	654, 717
8a	421(49.28), 518(2.04), 553(0.99), 592(0.50), 648 (0.35)	652, 717
8b	422(49.93), 517(1.97), 552 (0.92), 593(0.55), 648(0.38)	652, 718
8c	422(53.60), 518(2.51), 553(1.29), 593(0.66), 649(0.45)	652, 718
8d	422(51.26), 518(2.28), 553(1.19), 593(0.64), 649 (0.49)	652, 719
8e	421(46.64), 517(1.93), 553(0.92), 593(0.39), 648(0.17)	651, 716
9a	421(49.63), 517(2.09), 551(0.95), 593(0.53), 647(0.33)	651, 715
9b	421(50.25), 517(1.94), 551(0.82), 591(0.54), 646(0.38)	651, 717
9c	422(54.11), 517(2.45), 552(1.18), 593(0.69), 647(0.44)	651, 717
9d	421(52.13), 517(2.33), 552(1.15), 591(0.61), 647(0.36)	651, 717
11a	422(56.44), 429(61.94), 519(4.78), 552(2.01), 595(1.23), 651(0.92)	670, 722
11b	420(48.26), 517(3.39), 543(2.61), 585(1.26), 647(0.45)	651, 717
11c	425(41.05), 432(47.54), 557(3.18), 597(1.19)	621, 654

[a] Absorption and emission data were taken for $CHCl_3$ solutions of porphyrins at 298 K.
[b] The excitation wavelength for emission data is 420 nm.

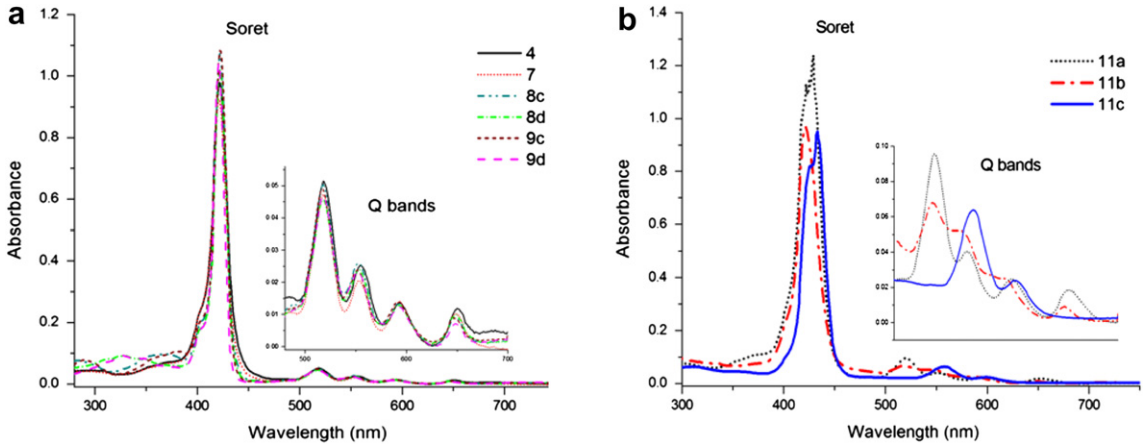

Fig. 1. (a) Electronic absorption spectra of porphyrins **4**, **7**, **8c**, **8d**, **9c** and **9d** in $CHCl_3$ at 298 K. (b) Electronic absorption spectra of *β*,*meso*-benzoxazolyl-bridged porphyrin dyads (**11a**–**c**) in $CHCl_3$ at 298 K. Inset in both (a) and (b) shows the Q bands.

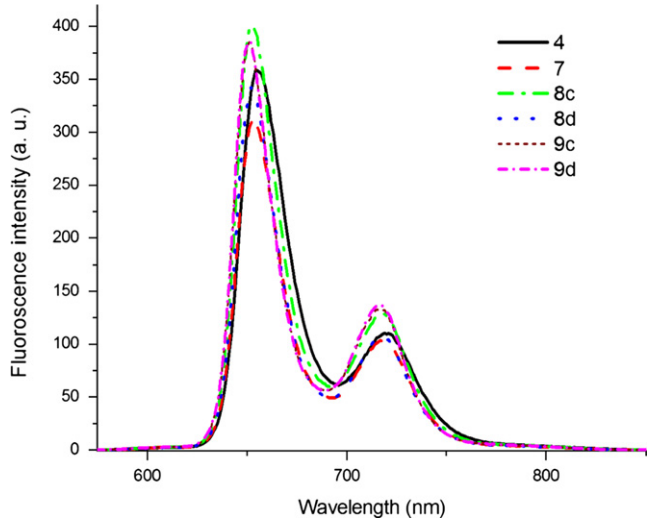

Fig. 2. Fluorescence spectra of porphyrins **4**, **7**, **8c**, **8d**, **9c** and **9d** in $CHCl_3$ (2×10^{-6} mol L^{-1}) at 298 K, $\lambda_{ex} = 420$ nm.

porphyrin dyad (**11a**) and 425, 432 nm for the zinc–zinc porphyrin dyad (**11c**), whereas the freebase–nickel complex (**11b**) exhibited only a Soret peak at 420 nm along with four broadened Q bands at 517, 543, 585 and 647 nm due to the overlapping of absorptions of freebase and nickel(II) porphyrin units. The splitting of Soret bands in the case of diporphyrins (**11a** and **11c**) possibly arises due to the non-planar deformation of the porphyrin core of *β*,*meso*-substituted component of the two compounds [37].

The fluorescence spectra of compounds **4**, **7**, **8c**, **8d**, **9c** and **9d** in $CHCl_3$ solution at excitation wavelength 420 nm are shown in Fig. 2. All these porphyrins showed typical emission bands at ~650 nm and a shoulder at ~717 nm with almost equal intensities. The fluorescence bands of the benzazolylporphyrins (**8c**–**d** and **9c**–**d**) are found to be blue-shifted by 3–4 nm in comparison to their corresponding precursors **4** or **7**, which suggests that there is no increment in the π-conjugation in these molecules. The energy transfer behavior of pyrene–porphyrin dyads (**8c** and **9c**) was studied by analyzing their absorption and emission spectra. Fig. 3a shows the emission spectra of pyrene-1-carboxaldehyde (**P-1**) and porphyrins (**4**, **7**, **8c** and **9c**) following 280 nm excitation. It was observed that the fluorescence of **P-1** at 420 nm due to the pyrene moiety is almost completely quenched on excitation of porphyrins **8c** and **9c** at 280 nm and there is an increase in the intensity of fluorescence band of these porphyrin dyads at ~652 and ~718 nm with respect to the starting porphyrin compounds **4** and **7**. Thus, it

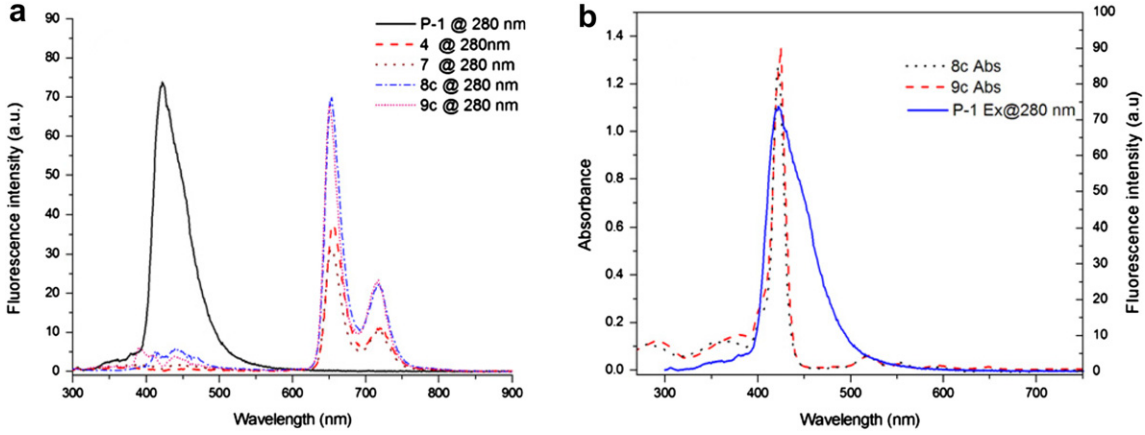

Fig. 3. (a) Emission spectra of **P-1** and porphyrins **4**, **7**, **8c** and **9c** in $CHCl_3$ (2×10^{-6} mol L^{-1}) at 298 K, $\lambda_{ex} = 280$ nm (b) UV–Vis spectra of **8c** and **9c** and fluorescence spectrum of **P-1** ($\lambda_{ex} = 280$ nm) in $CHCl_3$.

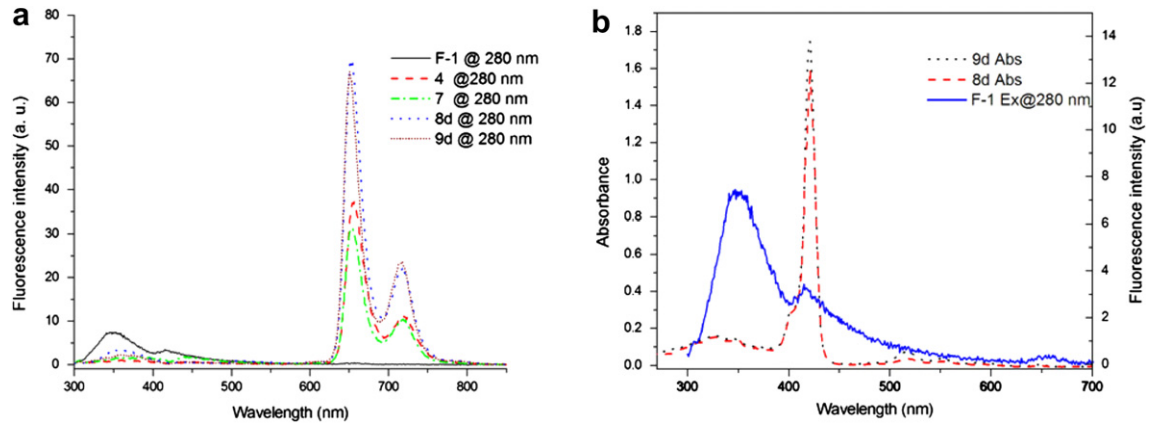

Fig. 4. (a) Fluorescence spectra of **F-1** and porphyrins **4**, **7**, **8d** and **9d** in $CHCl_3$ (2×10^{-6} mol L^{-1}) at 298 K, $\lambda_{ex} = 280$ nm (b) UV–Vis spectra of **8d** and **9d** and fluorescence spectrum of **F-1** ($\lambda_{ex} = 280$ nm) in $CHCl_3$.

shows that there is an efficient intramolecular energy transfer from the pyrene unit to the porphyrin ring in the dyads **8c** and **9c**. Further, the significant overlapping of fluorescence spectrum of **P-1** with the absorption spectra of **8c** and **9c** (Fig. 3b) also supports the above statement as it fulfills the first condition of energy transfer [38]. Similarly, the intramolecular energy transfer from the fluorene moiety to the porphyrin core was also observed in porphyrin–fluorene dyads **8d** and **9d** (Fig. 4a,b).

The fluorescence spectra of 5,10,15,20-tetraphenylporphyrin (TPP), zinc(II) 5,10,15,20-tetraphenylporphyrin (Zn-TPP) and *β*,*meso*-benzoxazolyl-bridged porphyrin dyads (**11a**–**c**) in chloroform solution at excitation wavelength 420 nm are presented in Fig. 5. The fluorescence spectra of diporphyrins (**11a**–**c)** showed two fluorescence bands at 670, 722 nm for freebase–freebase diporphyrin (**11a**), at 651, 717 nm for freebase-nickel(II) diporphyrin (**11b**) and at 621, 654 nm for zinc–zinc diporphyrin (**11c).** On excitation at 420 nm, the fluorescence bands of both diporphyrin **11a** and **11c** were significantly quenched and red shifted by ~20 nm with respect to TPP and Zn-TPP, respectively. In contrast, the strong emission quenching was observed in the case of diporphyrin (**11b**) at 651 and 717 nm with respect to TPP. These observations may be explained by the possible non-planarity of a component of the diporphyrins (**11a**–**c**) as the non-planar

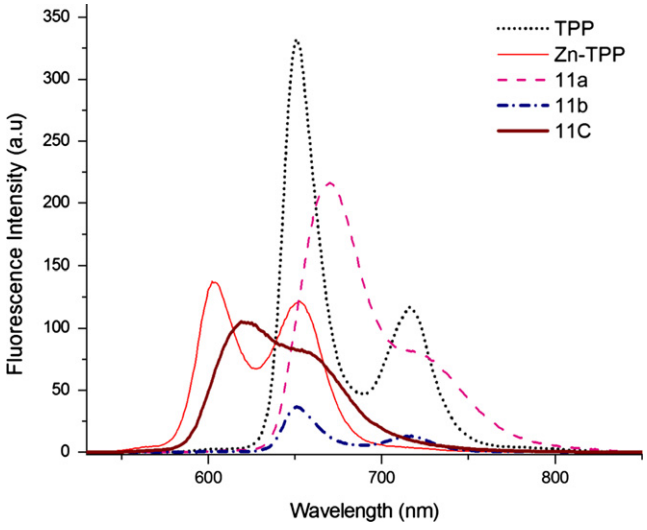

Fig. 5. Fluorescence spectra of **TPP**, **Zn-TPP** and **11a**–**c** in $CHCl_3$ (2×10^{-6} mol L^{-1}) at 298 K, $\lambda_{ex} = 420$ nm.

porphyrins are practically known to exhibit poor emission due to enhanced rates of internal conversion [39–42].

4. Conclusions

In summary, we have successfully synthesized and characterized two new porphyrin precursors, 5-(3,4-diaminophenyl)-10,15,20-triphenylporphyrin (**4**) and 5-(3-amino-4-hydroxyphenyl)-10,15,20-triphenylporphyrin (**7**), which can be used as starting materials for the synthesis of a variety of porphyrinic molecules and their metal complexes. To this end, a series of *meso*-substituted benzazolyl-triphenylporphyrins and *β*,*meso*-benzoxazolyl-bridged porphyrin dyads have been efficiently synthesized in good yields through $La(OTf)_3$-catalyzed condensation cyclization reaction of porphyrin **4** or **7** with various aromatic aldehydes. On photophysical investigation, a significant intramolecular energy transfer was observed from the pyrene and fluorene subunits to the porphyrin core in the case of porphyrins (**8c**–**d** and **9c**–**d**). Furthermore, the significant emission quenching observed in *β*,*meso*-benzoxazolyl-bridged porphyrin dyads (**11a**–**c**) was attributed to the possible non-planarity of synthesized diporphyrin macrocycles. These photophysical results are significantly encouraging and henceforth may be useful for designing new porphyrin molecules for various applications including light harvesting and photodynamic agents for photodynamic therapy.

Acknowledgments

We thank the University of Delhi, India for providing necessary financial support for this work. Satyasheel is grateful to Council of Scientific and Industrial Research, New Delhi, India for Senior Research Fellowship. The Jeol ECX 400P (400 MHz) NMR facility at USIC is acknowledged for NMR spectra.

References

[1] Zakavi S, Karimipour GR, Gharab NG. *Meso*-tetraarylporphyrin catalyzed highly regioselective ring opening of epoxides with acetic acid. Catalysis Communications 2009;10:388–90.
[2] Berkessel A, Erturk E, Laporte C. Chiral chromium(III) porphyrins as highly enantioselective catalysts for hetero-Diels–Alder reactions between aldehydes and dienes. Advanced Synthesis and Catalysis 2006;348:223–8.
[3] Lee C, Lee DH, Hong J-I. Colorimetric anion sensing by porphyrin-based anion receptors. Tetrahedron Letters 2001;42:8665–8.
[4] Starnes SD, Arungundram S, Saunders CH. Anion sensors based on *β*,*β*′-disubstituted porphyrin derivatives. Tetrahedron Letters 2002;43:7785–8.
[5] Zheng J-Y, Konishi K, Aida T. Guest-selective binding of z-amino acids by a strapped metalloporphyrin receptor with a hydrogen-bonding capability. Tetrahedron 1997;53:9115–22.

[6] Liang Y, Chang CK, Peng S-M. Molecular recognition with C-clamp porphyrins: synthesis, structural, and complexation studies. Journal of Molecular Recognition 1996;9:149–57.
[7] Nyman ES, Hynninen PH. Research advances in the use of tetrapyrrolic photosensitizers for photodynamic therapy. Journal of Photochemistry and Photobiology B: Biology 2004;73:1–28.
[8] Sternberg ED, Dolphin D, Bruckner C. Porphyrin-based photosensitizers for use in photodynamic therapy. Tetrahedron 1998;54:4151–202.
[9] Vicente MGH. Porphyrin-based sensitizers in the detection and treatment of cancer: recent progress. Current Medicinal Chemistry-Anti-Cancer Agents 2001;1:175–94.
[10] Wainwright M. Photodynamic therapy: the development of new photosensitizers. Anti-Cancer Agents in Medicinal Chemistry 2008;8:280–91.
[11] Imahori H. Porphyrin–fullerene linked systems as artificial photosynthetic mimics. Organic and Biomolecular Chemistry 2004;2:1425–33.
[12] Kuramochi Y, Sandanayaka ASD, Satake A, Araki Y, Ogawa K, Ito O, et al. Energy transfer followed by electron transfer in a porphyrin macrocycle and central acceptor ligand: a model for a photosynthetic composite of the light-harvesting complex and reaction center. Chemistry-A European Journal 2009; 15:2317–27.
[13] Wasielewski MR. Photoinduced electron transfer in supramolecular systems for artificial photosynthesis. Chemical Reviews 1992;92:435–61.
[14] Gust D, Moore TA, Moore AL. Mimicking photosynthetic solar energy transduction. Accounts of Chemical Research 2001;34:40–8.
[15] Holten D, Bocian DF, Lindsey JS. Probing electronic communication in covalently linked multiporphyrin arrays. A guide to the rational design of molecular photonic devices. Accounts of Chemical Research 2002;35:57–69.
[16] Gust D. Very small arrays. Nature 1997;386:21–2.
[17] Vicente MGH, Smith KM. Porphyrins with fused exocyclic rings. Journal of Porphyrins and Phthalocyanines 2004;8:26–42.
[18] Lembo A, Tagliatesta P, Guldi DM, Wielopolski M, Nuccetelli M. Porphyrin-β-oligo-ethynylenephenylene-[60]fullerene triads: synthesis and electrochemical and photophysical characterization of the new porphyrin-oligo-PPE-[60]fullerene systems. The Journal of Physical Chemistry A 2009;113:1779–93.
[19] Aihara H, Jaquinod L, Nurco DJ, Smith KM. Multicarbocycle formation mediated by arenoporphyrin 1,4-diradicals: synthesis of picenoporphyrins. Angewandte Chemie International Edition 2001;40:3439–41.
[20] Nath M, Huffman JC, Zaleski JM. Ambient temperature activation of haloporphyrinic-enediynes: electronic contributions to Bergman cycloaromatization. Journal of the American Chemical Society 2003;125:11484–5.
[21] Nath M, Pink M, Zaleski JM. Controlling both ground- and excited-state thermal barriers to Bergman cyclization with alkyne termini substitution. Journal of the American Chemical Society 2005;127:478–9.
[22] Nath M, Huffman JC, Zaleski JM. Accelerated Bergman cyclization of porphyrinic-enediynes. Chemical Communications; 2003:858–9.
[23] Jiao C, Huang K-W, Chi C, Wu J. Doubly and triply linked porphyrin–perylene monoimides as near IR dyes with large dipole moments and high photostability. The Journal of Organic Chemistry 2011;76:661–4.
[24] Tao M, Liu L, Liu D, Zhou X. Photoinduced energy and electron transfer in porphyrin-anthraquinone dyads bridged with a triazine group. Dyes and Pigments 2010;85:21–6.
[25] Drouet S, Paul-Roth CO, Simonneaux G. Synthesis and photophysical properties of porphyrins with fluorenyl pendant arms. Tetrahedron 2009;65:2975–81.
[26] Yang XG, Sun JZ, Li HY, Cao J, Wang M. Fluorescence switch based on a porphyrin–perylene dyad. Chinese Chemical Letters 2005;16(2):257–60.
[27] Kirmaier C, Song H-E, Yang E, Schwartz JK, Hindin E, Diers JR, et al. Excited-state photodynamics of perylene–porphyrin dyads. 5. Tuning light-harvesting characteristics via perylene substituents, connection motif, and three-dimensional architecture. The Journal of Physical Chemistry B 2010;114: 14249–64.
[28] Lin Z-M, Feng W-Z, Leung H-K. Photoinduced energy and electron transfer in pyrene–porphyrin, porphyrin–benzoquinone binary systems and the pyrene–porphyrin–benzoquinone ternary system. Journal of the Chemical Society, Chemical Communications; 1991:209–11.
[29] Yan X, Weng M, Zhang M, Shen T. Intermolecular and intramolecular energy and electron transfer reactions between porphyrin and fluorescein. Dyes and Pigments 1997;35:87–99.
[30] Sirish M, Maiya BG. Fluorescence studies on a supramolecular porphyrin bearing anthracene donor moieties. Journal of Photochemistry and Photobiology A: Chemistry 1995;85:127–35.
[31] Shinokubo H, Osuka A. Marriage of porphyrin chemistry with metal-catalysed reactions. Chemical Communications; 2009:1011–21.
[32] Susumu K, Duncan TV, Therien MJ. Potentiometric, electronic structural, and ground- and excited-state optical properties of conjugated bis[(porphinato) zinc(II)] compounds featuring proquinoidal spacer units. Journal of the American Chemical Society 2005;127:5186–95.
[33] Zhou X, Chan KS. Synthesis of β-linked diporphyrins and their homo- and hetero-bimetallic complexes. The Journal of Organic Chemistry 1998;63: 99–104.
[34] Zhang H-L, Shi W-M, Wu J. Regiospecific aryl nitration of *meso*-tetraarylporphyrins: the directive effect of para-substituents. Heterocycles 2005; 65(12):3001–6.
[35] Xue Z, Kwong DW-J, Xue L-W, Liu Q, Hou A-X, Wong W-K. Synthesis of novel diselenide-linked porphyrin dimers under phase-transfer catalysis condition and their interactions with DNA. Chemistry & Biodiversity 2009;6:1131–43.
[36] Meot-Ner M, Adler AD. Substituent effects in noncoplanar π systems. *ms*-Porphins. Journal of the American Chemical Society 1975;97:5107–11.
[37] Haddad RE, Gazeau S, Pecaut J, Marchon J-C, Medforth CJ, Shelnutt JA. Origin of the red shifts in the optical absorption bands of nonplanar tetraalkylporphyrins. Journal of the American Chemical Society 2003;125:1253–68.
[38] Leibowitz M. Remarks on Förster's theory of transfer of excitation energy. The Journal of Physical Chemistry 1965;69:1061–2.
[39] Sazanovich IV, Galievsky VA, Hoek AV, Schaafsma TJ, Malinovskii VL, Holten D, et al. Photophysical and structural properties of saddle-shaped free base porphyrins: evidence for an "orthogonal" dipole moment. The Journal of Physical Chemistry B 2001;105:7818–29.
[40] Gentemann S, Medforth CJ, Forsyth TP, Nurco DJ, Smith KM, Fajer J, et al. Photophysical properties of conformationally distorted metal-free porphyrins. Investigation into the deactivation mechanisms of the lowest excited singlet state. Journal of the American Chemical Society 1994;116:7363–8.
[41] Charlesworth P, Truscott TG, Kessel D, Medforth CJ, Smith KM. Photophysical studies of substituted porphyrins. Journal of the Chemical Society, Faraday Transactions 1994;90:1073–6.
[42] Gentemann S, Medforth CJ, Ema T, Nelson NY, Smith KM, Fajer J, et al. Unusual picosecond $^1(\pi, \pi^*)$ deactivation of ruffled nonplanar porphyrins. Chemical Physics Letters 1995;245:441–7.